Double-Sided Ion Thruster for Contactless Space Debris Removal: Experimental Results

IEPC-2017-261

Presented at the 35th International Electric Propulsion Conference
Georgia Institute of Technology • Atlanta, Georgia • USA
October 8 – 12, 2017

M. Dobkevicius[1]
University of Southampton, Southampton, SO17 1BJ, UK

M. Smirnova[2], A. M. Perez[3]
TransMIT Gmbh, Giessen, 35394, Germanys

and

D. Feili[4]
ESTEC (ESA), Noordwijk, 2201, Netherlands

The Ion Beam Shepherd (IBS) space debris removal method requires two thrusters: one for impulse transfer (IT) and one for impulse compensation (IC). This paper proposes a novel thruster concept for the IBS type missions where a single Double-Sided Thruster (DST) simultaneously producing ion beams for the IT and IC purposes is used. The advantage of DST design is that it requires approximately half the RF power compared with two single-ended thrusters and it has a much simpler sub-system architecture, lower cost, and lower total mass. Such a DST thruster was designed, built and tested, with the requirements and constraints taken from the LEOSWEEP space debris removal mission. During the experimental campaign, a successful extraction of two ion beams was achieved. The paper shows that it is possible to independently control the thrust magnitudes from the IT and IC thruster sides by varying the number of apertures in each ion optics system and by altering accel grid voltages, proving that the DST concept is a viable alternative for the LOESWEEP mission.

Nomenclature

F	=	thrust, N
n	=	density, $1/m^3$
P	=	power, W
S	=	area, m^2
U	=	voltage, V

I. Introduction

Ion Beam Shepherd (IBS) has been suggested as one of the possible methods to target the space debris problem.[1,2] As a result, the LEOSWEEP (Improving Low Earth Orbit Security with Enhanced Electric Propulsion) mission

[1] PhD student, Aeronautics & Astronautics, (currently at Agilent Technologies), mantasdb@gmail.com.
[2] Electric propulsion engineer, maria.smirnova@transmit.de.
[3] Electric propulsion engineer, aloha.mingo@transmit.de.
[4] Electric propulsion engineer, Davar.Feili@esa.int.

plans to use the IBS method to de-orbit a 1.5-ton launcher upper stage from a nearly polar low Earth orbit (LEO).[3] To successfully perform the mission, two thrusters are needed. In addition, the mission requires that the thrust delivered to the target is more than 30 mN and the total power of both thrusters is less than 3 kW.[4] However, such a two-thruster design introduces a lot of complexity regarding the power and propellant management systems. To help mitigate these issues associated with the two-thruster design, a novel ion thruster concept for the IBS type missions was presented in our previous works.[5,6] This concept, instead of using two thrusters, requires only one thruster capable of generating two distinct ion beams for the impulse transfer (IT) and impulse compensation (IC) purposes. The advantage of such a design is that it potentially requires about two times less RF power than two single-ended thrusters. Additionally, it is expected that such a system would have a much simpler sub-system architecture, lower cost, and lower total mass. In the paper, the concept thruster is referred to as the Double-Sided Thruster (DST). The DST thruster has been designed and optimized using the RF gridded ion thruster model developed in our previous work[7] while keeping the LEOSWEEP mission concept requirements as constraints. Once designed, the DST was manufactured, assembled and tested. In this paper, we present results from the experimental DST test campaign.[6]

Figure 1 shows a detailed view of the DST concept. In particular, Figure 1 indicates the main power supplies required for the thruster, the electrical scheme and the main performance parameters/relations. As mentioned above, one side of the thruster is used to produce the impulse transfer thrust F_{IT}, while the other side is used to produce the impulse compensation thrust F_{IC}. To create the plasma, the power P_{in} is fed to the coil using the RFG and the propellant is supplied into the discharge chamber. The plasma is extracted by applying the potential U_s on the screen grid and the negative potential U_{a1} on the acceleration (accel) grid. Since the applied screen voltage on the IT side shows up in the plasma sheath itself, it means that the same floating potential will be present on the screen grid at the IC side of the thruster as well. Therefore, to extract the beam from the IC side, it is enough to apply the voltage U_{a2} on the accel grid at the IC side. The total power to the thruster P_{tot} is then composed of the RFG power P_{in} and the two beam powers P_{b1} and P_{b2}.

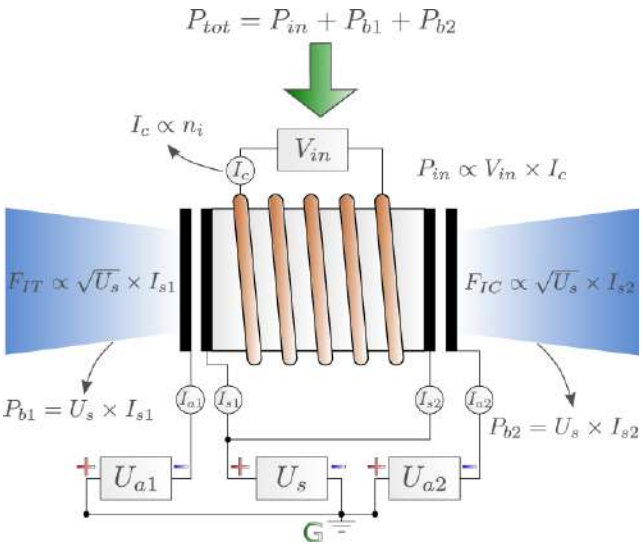

Figure 1. Double-sided ion thruster electrical circuit schematic, main performance parameters and relations.

Note that even though the screen voltage is the same for both sides, the beam powers differ based on the extracted currents I_{s1} and I_{s2} from the IT and IC sides, respectively. Furthermore, as seen in Figure 1, the thrust magnitudes F_{IT} and F_{IC} are proportional to the screen grid voltage U_s. This means that the thrusts generated from each side of the thruster are coupled. That is, for a constant RFG power and propellant flow rate, the thrust magnitude produced by each set of grids is dependent on the screen grid voltage U_s. This is because the plasma potential is common to both ion extraction systems. Therefore, it becomes challenging to independently control the thrust values from the IT and IC sides. For instance, this could cause various issues if a large (and variable) difference between the F_{IT} and F_{IC} values is required. There are a few possible ways to control the thrust magnitudes from the IT and IC sides independently, which is necessary to meet the LEOSWEEP mission requirements.

The first way is to adjust the I_{s1} and I_{s2} currents extracted from the IT and IC sides, respectively. This can be done by manufacturing the ion optics systems with the pre-defined number *N* of apertures with the area *S*, as illustrated in Figure 2(a). The thrust values can be controlled using the following relations

$$\frac{F_{IC}}{F_{IT}} \propto \frac{I_{s2}}{I_{s1}} \propto \frac{N_{IC}S_{IC}n_iU_s}{N_{IT}S_{IT}n_iU_s} \propto \frac{N_{IC}S_{IC}}{N_{IT}S_{IT}},$$

where N_{IT} and N_{IC} are the number of apertures in the ion optics systems of the IT and IC sides, respectively. Whereas, S_{IT} and S_{IC} are the aperture areas in the ion optics systems of the IT and IC sides, respectively. As can be seen from the above equation, since the ion density n_i and the screen grid voltage U_s are common to both ion optics systems, they cancel each other out. Therefore, the thrust ratio F_{IC}/F_{IT} can be controlled by adjusting the total grid extraction area of each ion optics system. Note that the ion density does vary along the length of the discharge chamber. However, this variation is usually symmetric around the center of the discharge chamber, meaning that ion densities at both ends of the discharge chamber are roughly equal.[8]

Another way to independently control the thrust values is by modifying the plasma meniscus shape at the either ion optics system, as depicted in Figure 2(b). This can be achieved by varying the accel voltages U_{a1} and U_{a2}. The change in the plasma meniscus shape modifies the ion optics effective transparency T_s, which in turn affects the extracted currents I_{s1} and I_{s2}. As was proven earlier, this causes a change in the F_{IT} and F_{IC} thrust values. However, the change in the extracted current due to the change in the meniscus shape is expected to be very small. Therefore, this method of thrust control is only suitable for very fine thrust adjustments that might be required during the mission. Both methods of the thrust control were investigated experimentally, and the results from the investigation are presented in the following sections.

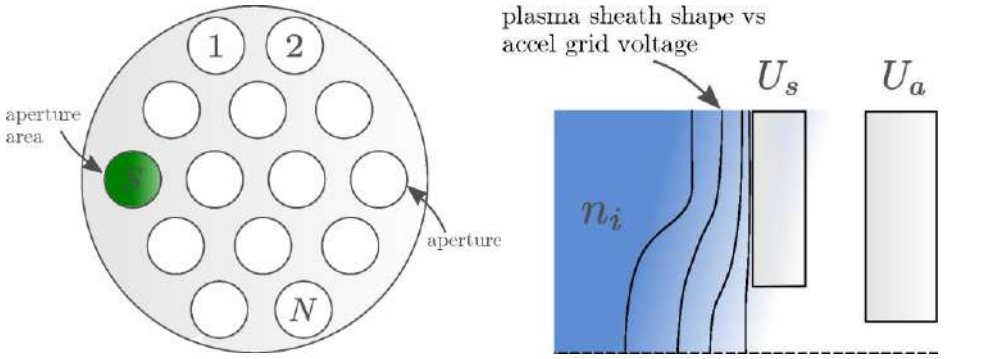

a) Ion optics geometry. **b) Accel grid voltage effect on plasma sheath.**

Figure 2. Phenomena affecting the ion beam current.

II. Experimental campaign

A. Double-sided thruster

1. Design

The double-sided ion thruster has been designed, manufactured and assembled. The design and optimization of the thruster were driven by the computational tools developed in Refs. 6 and 7. In performing the optimization analysis, the coil number of turns *N* and discharge chamber length *l* were varied with the goal to reduce the total input power. The parameters of the LEOSWEEP mission were taken as constraints while performing the optimization. In particular, it was assumed that 30 mN of thrust must be transferred to the debris target, the mass flow rate is 15 sccm and the screen grid voltage is 3 kV. Furthermore, it was assumed that the discharge chamber diameter is fixed at about 17 cm. This is because it was decided to use the ITT[9] ion optics system, which has an active diameter of about 16 cm, for the IT side of the DST. Also, the coil diameter was set to 4.5 mm due to the capability of obtaining a copper tube of this diameter. Based on the optimization results, it was decided to choose a chamber length of about 80 mm and the coil with *N/l* of about 0.1, which would translate into 8 turns. The CAD drawings of the cross-sectional views of the DST

with final dimensions are shown in Figure 3. As can be seen from Figure 3, the discharge chamber length is 7.67 cm and the coil has 8 turns. What is more, the thruster was designed in such a way that it could be set up in two configurations depending on the type of the ion optics system used for the IC side.

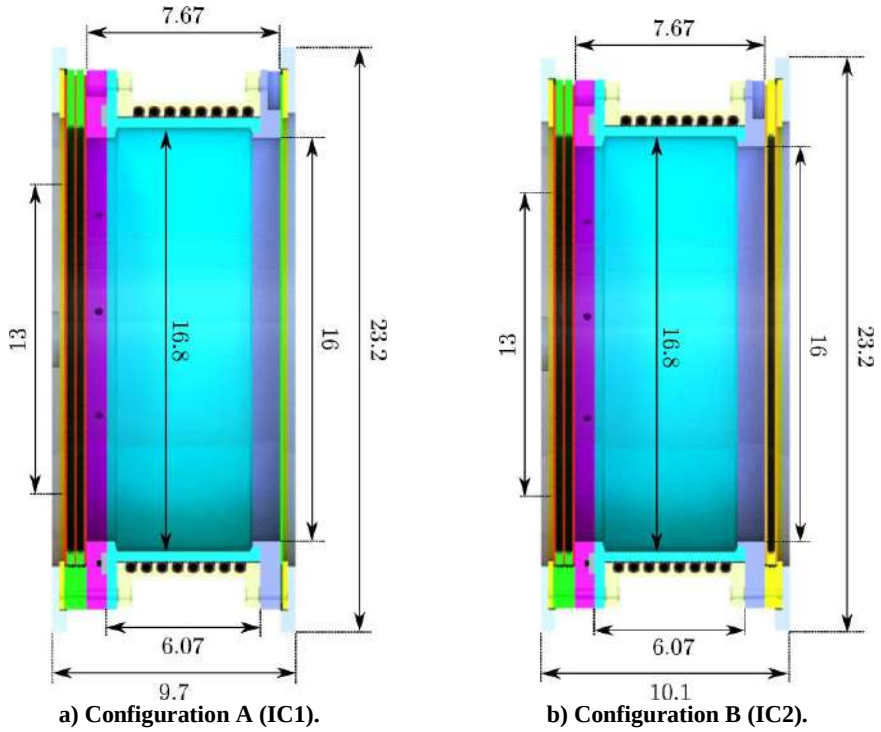

a) Configuration A (IC1). **b) Configuration B (IC2).**

Figure 3. CAD drawings of the cross-sectional views of the DST thruster for Configuration A and Configuration B. All dimensions are in cm.

In Configuration A, an IC1 ion optics system composed of a single grid was used for the IC side. Whereas, in Configuration B, an IC2 ion optics system composed of two grids was employed for the IC side. In both A and B Configurations, for the IT side, an IT ion optics system having three grids was used. As Figure 3 depicts, both configurations have a single discharge chamber and a single coil. What is more, the IT ion optics and the IC1 ion optics systems are located on the left and right sides of the discharge chamber, respectively. Furthermore, Configuration B has the IC2 ion optics system on the right side of the discharge chamber. Notice that both configurations are nearly identical in terms of thruster's dimensions. Nevertheless, in Configuration B, the thruster is 0.4 cm wider to accommodate for the additional grid on the IC side.

2. Configuration A and Configuration B

Figure 4 shows the DST thruster in Configuration A from both the IT and IC ion optics sides. Figure 4 also indicates the main components of the thruster and the materials. Note that the IT ion optics has three grids that are all made from carbon-carbon (C-C) material. Each C-C grid has 948 apertures, and the screen grid aperture diameter is 2.8 mm. Also, observe that the IT ion optics system has an area at the center that has no apertures and there is a hole at the center as well. To be able to use the IT ion optics system in the DST thruster, the hole was taped with an aluminum (Al) tape, as seen in Figure 4(a). This is because the IT ion optics system was taken from the ITT[9] thruster, and the hole was used to house the neutralizer. As depicted in Figure 4(b), the IC1 ion optics has apertures throughout the area of the grid. The grid itself is made from SILUX[10] and has a layer of aluminum taped on the accel side. The SILUX grid has 1171 2 mm diameter apertures. Observe that the gas inlet locations are different between the two configurations. This is because, initially, the gas inlet was located as shown in Figure 4(b). However, to prevent sparks from forming between the gas inlet and the beam, the gas inlet was installed as depicted in Figure 4(a).

Finally, observe from Figure 4 that in Configuration A, the thruster has four electrodes: IT screen (I_{s1}), IT accel (I_{a1}), IT GND and IC accel I_{a2}). Figure 4 illustrates that all electrode connections are made using safe high voltage (SHV) connectors. Similarly, Figure 5 depicts the DST thruster in Configuration B. As was discussed previously, Configuration B has a different IC ion optics system represented with two titanium (Ti) grids and denoted as IC2. Each titanium grid has 1171 2 mm diameter apertures. Furthermore, there is also an additional IC accel electrode (I_{a2}) that is connected to the power supply directly through a cable. What is more, on the IT side, the SHV connector is no longer used as the IC accel (I_{a2}) electrode. It is now employed to provide the screen potential, and it acts as the IC screen (I_{s2}) electrode. Note that all other geometrical parameters between the two configurations are nearly exactly the same, as was discussed in the previous section.

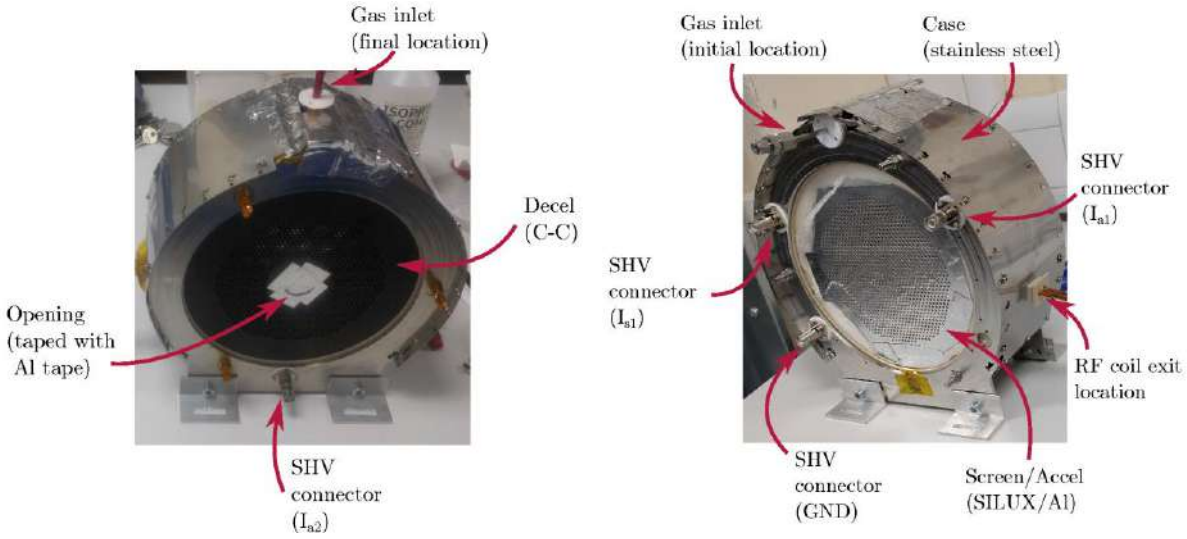

a) IT ion optics. **b) IC1 ion optics.**

Figure 4. IT and IC ion optics sides in Configuration A.

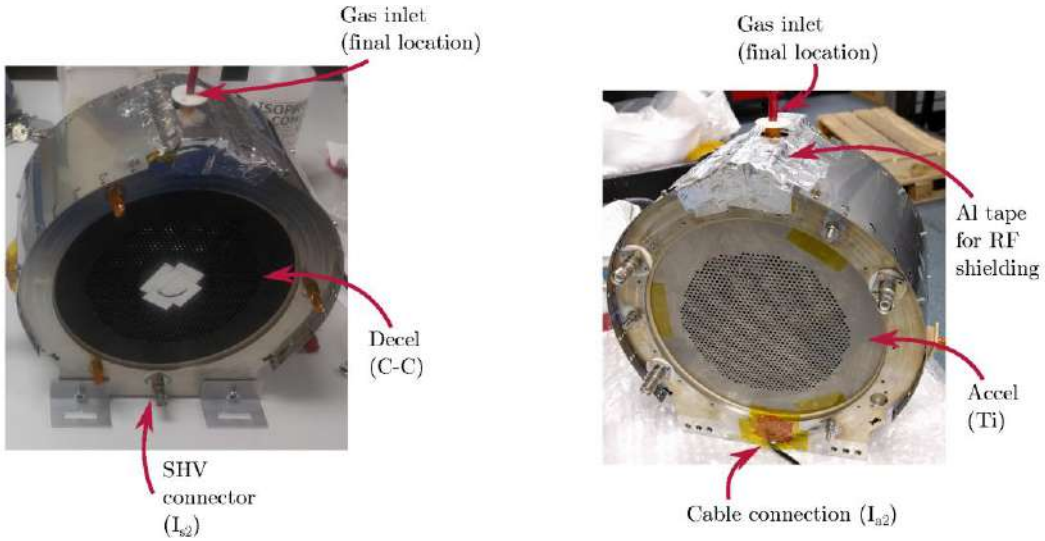

a) IT ion optics. **b) IC2 ion optics.**

Figure 5. IT and IC ion optics sides in Configuration B.

B. Experimental set-up

1. *Configurations*

The DST was designed in such a way that it could be tested in multiple configurations. The figures below describe the type of the ion optics system used and the electrical set-up of each configuration. Figure 6 shows Configuration A. In Configuration A, the thruster uses a combination of the IT and IC1 ion optics systems. Additionally, depending on which ion optics side is active, Configuration A can be run in three different modes. The first two modes are called AIT and AIC. In these modes, either the IT or IC side of the ion optics is blocked with Kapton tape, respectively. Therefore, the ion beam is extracted only from the active side. Such a configuration is useful when testing the performance of the IT or IC ion optics side only. This helps gauging the thruster's, especially the ion optics, design and efficiency. Figure 6 also illustrates the electrical set-up of Configuration A. First, observe that the current I_c, supplied using the RFG, flows in the coil. Additionally, the screen grid is connected to the SCREEN (U_s) power supply, while the accel grid is connected to the ACCEL1 (U_{a1}) power supply. The decel grid is grounded. Furthermore, there are current measuring devices (A) installed in the SCREEN and ACCEL lines.

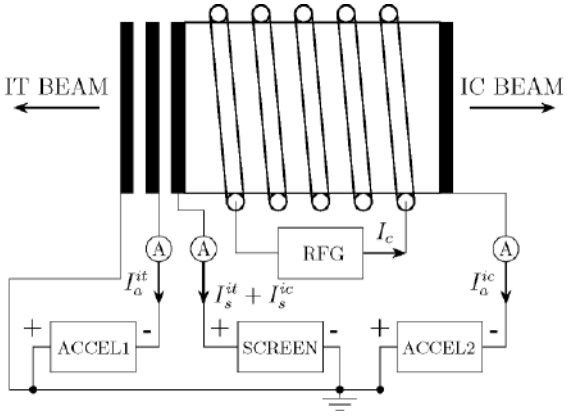

Figure 6. Configuration A: AIT – IT beam active, AIC – IC beam active, ADST – IT and IC beams active.

Notice that since the IC1 ion optics does not have a screen grid, the screen potential is provided using the SCREEN power supply connected to the screen grid of the IT ion optics system. Also, the aluminum tape on the IC1 grid is connected to the ACCEL2 (U_{a2}) power supply. Technically speaking, the current I_s^{ic} that is measured by the SCREEN power supply is not the actual current falling on the screen grid of the IC1 ion optics system since, as mentioned before, the IC1 ion optics system does not have a screen grid. Instead, I_s^{ic} is the electron current equivalent to the ion current that is extracted by the IC1 ion optics system. However, for clarity, the term "screen current" is still used when talking about the IC1 ion optics system throughout the paper.

Finally, to check if the thruster could be run in the double-sided mode, both ion optics systems were opened. Such an operational condition is called Configuration ADST. In Configuration ADST, as before, only a single RFG power supply is used. Note that since there is no screen grid on the IC side, the extracted currents from the IT side (I_s^{it}) and the IC side (I_s^{ic}) are processed by the SCREEN power supply. Therefore, the SCREEN power supply shows a sum I_s^{it}+I_s^{ic} of the two currents. As a result, it is not possible to know the exact currents I_s^{it} and I_s^{ic} that are extracted from each side individually without performing the beam plume measurements using probes. Moreover, the current I_a^{it} shows the ion current falling on the accel grid of the IT ion optics, while the current I_a^{ic} represents the ion current hitting the conductive aluminum layer on the IC1 grid.

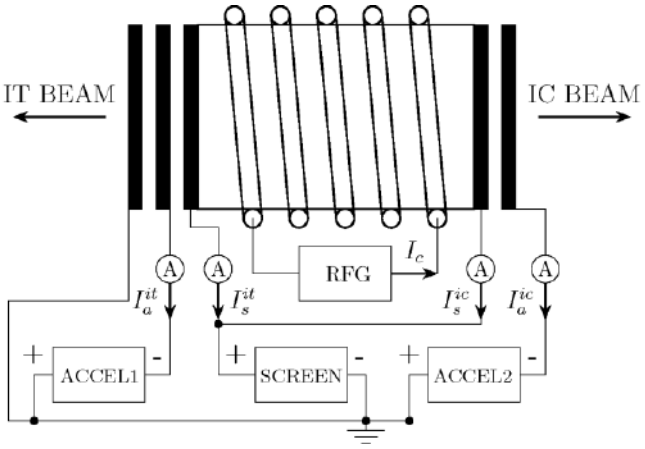

Figure 7. Configuration B: BDST- IT and IC beams active.

Furthermore, Configuration B represents the DST thruster with a combination of the IT and IC2 ion optics systems. However, in Configuration B, the thruster is tested only in the double-sided mode. That is, both ion optics systems are active and two ion beams are simultaneously extracted from the IT and IC sides, as shown in Figure 7. The IC2 ion optics system does have a screen grid. Therefore, the current I_s^{ic}, that represents the actual electron current hitting the screen grid, is measured in the line connected to the SCREEN power supply. However, note that the SCREEN power supply still displays the sum of both currents. Configuration B allows tracking precisely how the I_s^{it} and I_s^{ic} currents change while varying the SCREEN/ACCEL voltages, RFG power and gas flow rate. This, in turn, enables the thrust values from each side to be determined.

2. Vacuum facility

The thruster was tested at the University of Southampton vacuum facility shown in Figure 8. The facility consists of a test chamber and a loading chamber separated by a pneumatic, high vacuum isolation gate valve. The test chamber has a diameter of about 1.9 m and a total length of about 4 m. Whereas, the loading chamber is approximately 0.75 m in diameter and length. The main test chamber can reach the base pressure in the range of 10^{-8} mbar using a combination of two turbopumps backed by a rough pump and two cryopanels. Note that the DST thruster was tested only in the main chamber, with the vacuum isolation valve closed.

Figure 8. Outside view of the University of Southampton vacuum test facility.

The generation of vacuum from atmospheric conditions in the test chamber takes place in a two-stage pumping procedure. First, a water cooled, dry compression screw pump (Oerlikon Leybold LV140C) is utilized to reach a pressure equal to about 10^{-2} mbar. Once a sufficient pressure is achieved, the rough pump starts acting as a backing pump. Then, two magnetically-levitated turbo molecular pumps (Oerlikon Leybold MAG W 2200 iP) are turned on

to reach an ultimate pressure of about 10^{-8} mbar (with cryopanels on). The pressure in the test chamber is monitored by a combination of Pirani and cold cathode gauges. The main equipment that was used in the test set-up for the DST thruster is shown in Figure 9. As indicated in Figure 9, the test set-up consists of the following components: electrical power supplies for the ion optics, electrical power supplies for the RFG, data measuring/monitoring devices and a propellant management system.

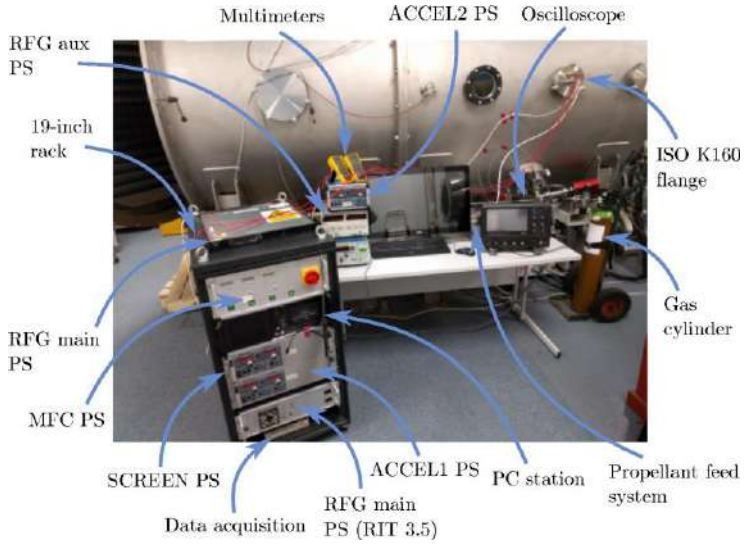

Figure 9. Overview of the DST thruster's set-up outside the vacuum facility.

The way the DST was installed on the support structure is shown in Figure 10. In particular, Figure 10(a) depicts the installation from the IC side. As can be seen, the RFG was installed directly underneath the thruster using two rails attached to the support structure. The DST thruster itself was attached using L-shaped aluminum brackets. One side of the bracket was attached to the rail of the support structure, while the other side was secured to the DST thruster's case which had 5 mm diameter holes drilled in. Note that the thruster's support structure was grounded. Therefore, the decel grid was connected directly to the thruster's support structure. Furthermore, the IT side of the thruster is shown in Figure 10(b). As Figure 10(b) illustrates, the thruster was placed approximately in the middle of the test chamber since there were two ion beams coming from the thruster. The beam from the IT side was directed towards the graphite beam target, while the beam from the IC side was aimed towards a concave stainless-steel sheet.

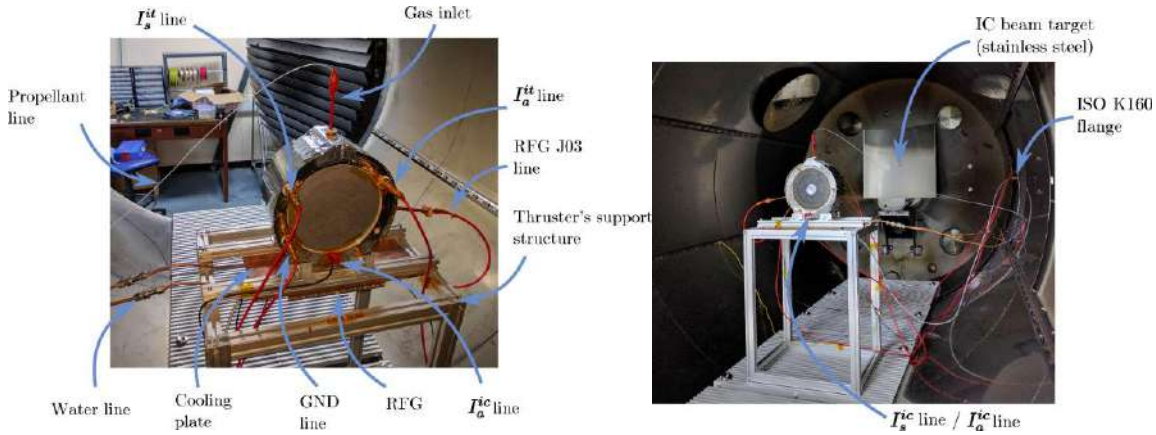

a) IC side. **b) IT side.**

Figure 10. DST installation when in Configuration BDST from the IT and IC sides inside the main chamber of the vacuum facility.

III. Experimental results

A. Configuration ADST

1. Performance mapping

The experimental results have been performed as a part of the PhD thesis[6]. Only the main results are presented in the paper. The data measured during the experimental campaign are summarized in Ref. 11. This section presents the performance mapping results for Configuration ADST. In this configuration, both the IT and IC ion optics systems are active and therefore there are two ion beams being extracted from each side, as shown in Figure 11. First, notice that since the view port was facing towards the IC side, the beam from the IC side appears much brighter than that from the IT side. Also, the IC1 ion optics system is semi-transparent to light from the plasma. In Configuration ADST, the thruster was tested with mass flow rates ranging from 6 to 14 sccm in 1 sccm increments. Figure 12(a) displays the total screen grid current (expressed as I_s^{it}+I_s^{ic}) which is collected by the IT side screen grid. Note that the screen grid current in Configuration ADST is roughly equal to a sum of the screen currents obtained in Configurations AIT and AIC where only a single ion optics side was active. This is because in Configuration ADST both ion optics systems are active and therefore there are two ion beams. As can be inferred from Figure 12(a), the maximum total screen grid current is about 200 mA at around 102 W and 11 sccm. This means that, for the same RFG power, the total extracted screen current can be roughly obtained by summing the I_s^{it} and I_s^{ic} currents. Note, however, that the mass flow rate must be doubled in the double-sided mode.

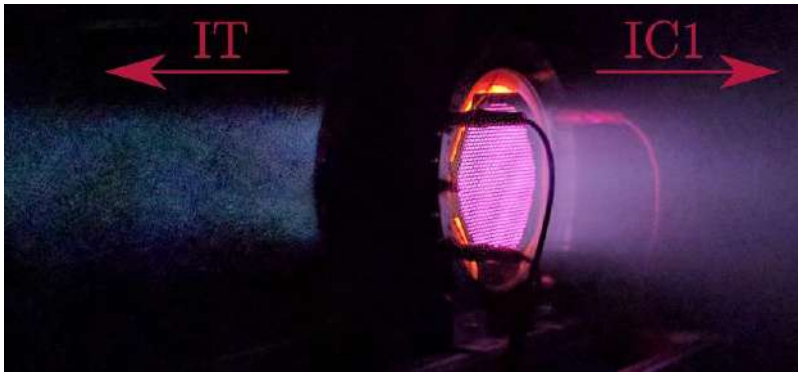

Figure 11. Extracted ion beams from the IT and IC1 ion optics systems in Configuration ADST.

Since in Configuration ADST the accel grids from the IT and IC sides are both collecting currents, the results for each side are plotted individually. Figure 12(b) and Figure 12(c) display how the accel currents I_a^{it} and I_a^{ic} vary with the RFG power, respectively. As can be observed from the figures, the IT and IC accel currents are similar in magnitude, especially at higher RFG powers. For example, at 14 sccm, the IT accel current is 2.3 mA, while the IC accel current is 2.4 mA. Nevertheless, since the IC side extracts a larger beam current, a percentage of the extracted current hitting the accel grid is smaller in the case of the IC side in comparison to the IT side. However, as mentioned before, due to the IC1 grid being made from a non-conductive material, it is not possible to know the exact current hitting the grid. Additionally, the IC accel current is about 20% lower than the IT accel current at low RFG powers. For instance, at 14 sccm and 45 W of RFG power, the IT accel current is nearly 0.8 mA, while the IC accel current at the same conditions is about 0.6 mA.

Figure 12(d) depicts the RFG current variation with the RFG power. As Figure 12(d) indicates, even though the mass flow rates in Configuration ADST are two times higher, the RFG current is approximately the same as was observed in the single-sided cases AIT and AIC. This means that the plasma inside the discharge chamber is of about the same pressure and density. Therefore, a conclusion can be drawn that adding an additional extraction system does not substantially change the plasma parameters if the mass flow rate (or the neutral gas pressure) into the discharge chamber is kept the same.

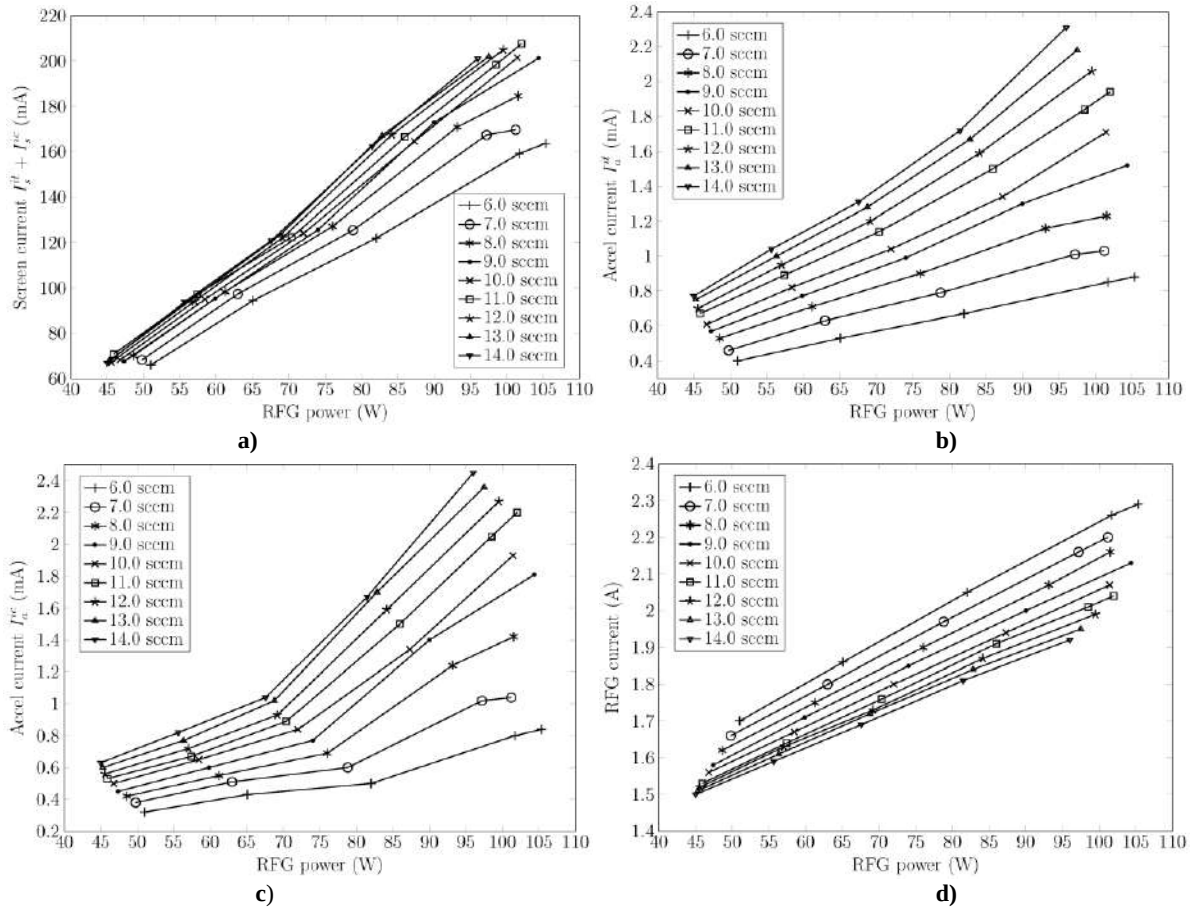

Figure 12. Configuration ADST: performance mapping at U_s=1.5 kV, U_{a1}=-250 V, U_{a2}=-200 V.

2. Performance analysis

In the performance analysis section, the performance parameters are plotted for the thruster as a whole, that is, when both ion optics sides are active. Note that when analyzing the thruster's performance in the double-sided mode, it is assumed that the thruster behaves as two individual thrusters. That is, the total thrust is defined as $T = T^{it} + T^{ic}$, while the total beam current is defined as $I_b = I_b^{it} + I_b^{ic}$. These definitions of thrust and beam current are then used to calculate the discharge loss, specific impulse and other performance parameters. This was done to have the double-sided thruster's performance easily comparable to the performance of single-sided thrusters. As can be seen in Figure 13(a), the discharge loss is about 650 W/A at 6 sccm and 0.4 mass utilization efficiency. Such a discharge loss is almost two times lower compared to Configurations AIT and AIC. This comes from the fact that in Configuration ADST, two ion beams are being extracted for roughly the same RFG power. The trend behavior, however, is about the same as for the single-sided cases. Also, the highest achievable mass utilization efficiency in Configuration ADST is approximately the same as for the single-sided cases and equal to 0.4. Similarly, the maximum specific impulse is equal to approximately 1,800 s, as seen in Figure 13(b). This is because even though two ion beams are being extracted in Configuration ADST, the mass flow rate is about two times higher as well. Therefore, the specific impulse does not improve in Configuration ADST.

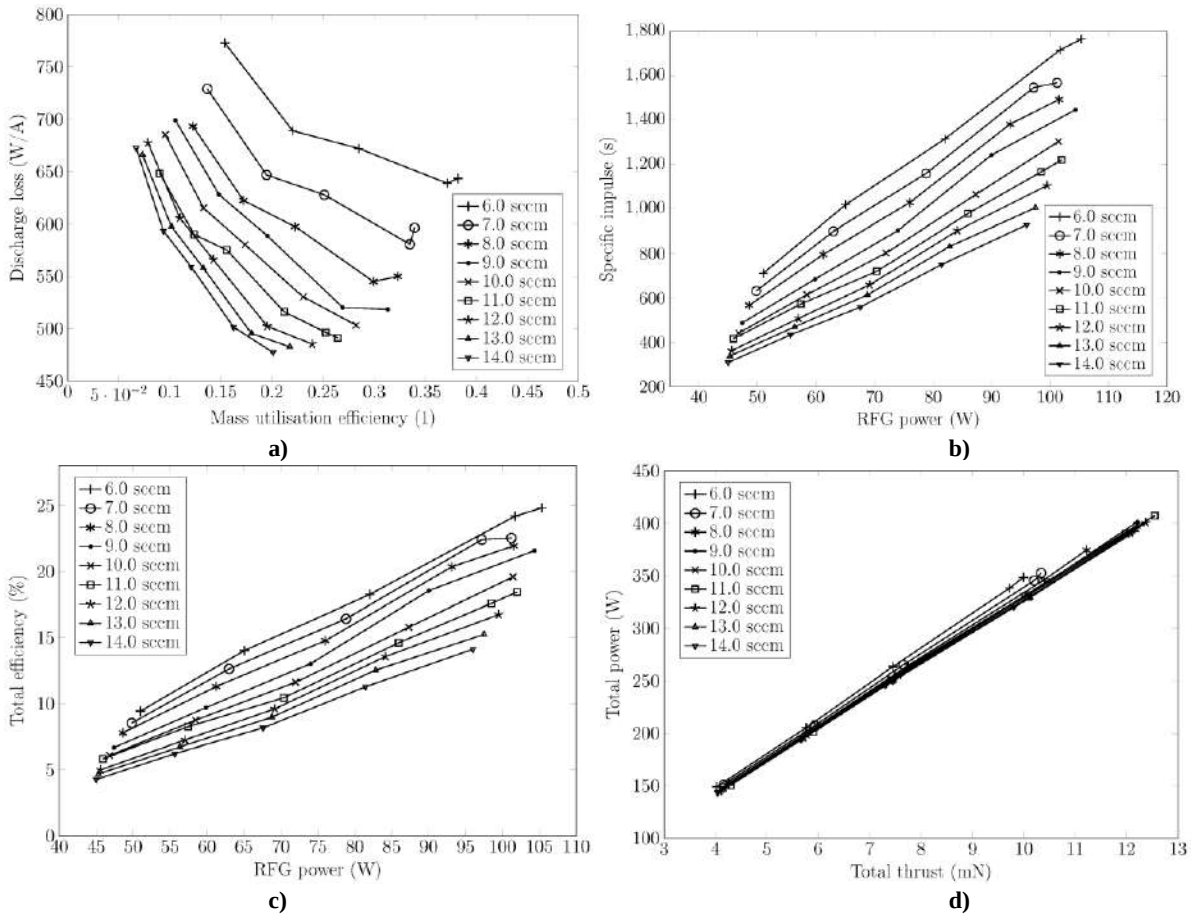

Figure 13. Configuration ADST: performance analysis at U_s=1.5 kV, U_{a1}=-250 V, U_{a2}=-200 V.

From Figure 13(c), the total efficiency of the thruster is still approximately the same as for the single-sided cases. This is because the total efficiency is determined mostly by the design of the thruster, that is, the coil shape and discharge chamber geometry. Since these parameters were kept the same, the total efficiency remained about the same as well even though two ion beams were extracted. Finally, Figure 13(d) displays the total power variation with the thrust. The thrust that is plotted in Figure 13(d) is obtained by using the total screen current from the IT and IC sides, as has been shown in Figure 12(a). Remember that the IC ion optics side does not have a screen grid. Therefore, it is not possible to estimate the thrust produced by each side individually. However, in Configuration ADST, the thrust is about double that compared to the single-sided cases. Note that the total power also has increased. This is because even though the RFG power remains the same in the double-sided mode, the beam power increases nearly twofold due to the production of two ion beams.

3. Performance comparison

The issue with having only one screen grid at the IC side, as in Configuration ADST, is that it is not possible to determine how much thrust is produced from the IT and IC sides independently without doing the beam plume measurements. Additionally, since the IT and IC1 ion optics systems are different, it cannot be said that the thruster's performance at 10 sccm in Configuration ADST is equivalent to a sum of the performance parameters at 5 sccm in Configuration AIT and 5 sccm in Configuration AIC. However, the results based on the equivalent mass flow rates from Configurations AIT and AIC could be used to estimate the thrust produced from the IT and IC sides independently in Configuration ADST. To do so, a combination of mass flow rates has to be found that produces a similar neutral gas pressure inside the discharge chamber as in Configuration ADST.

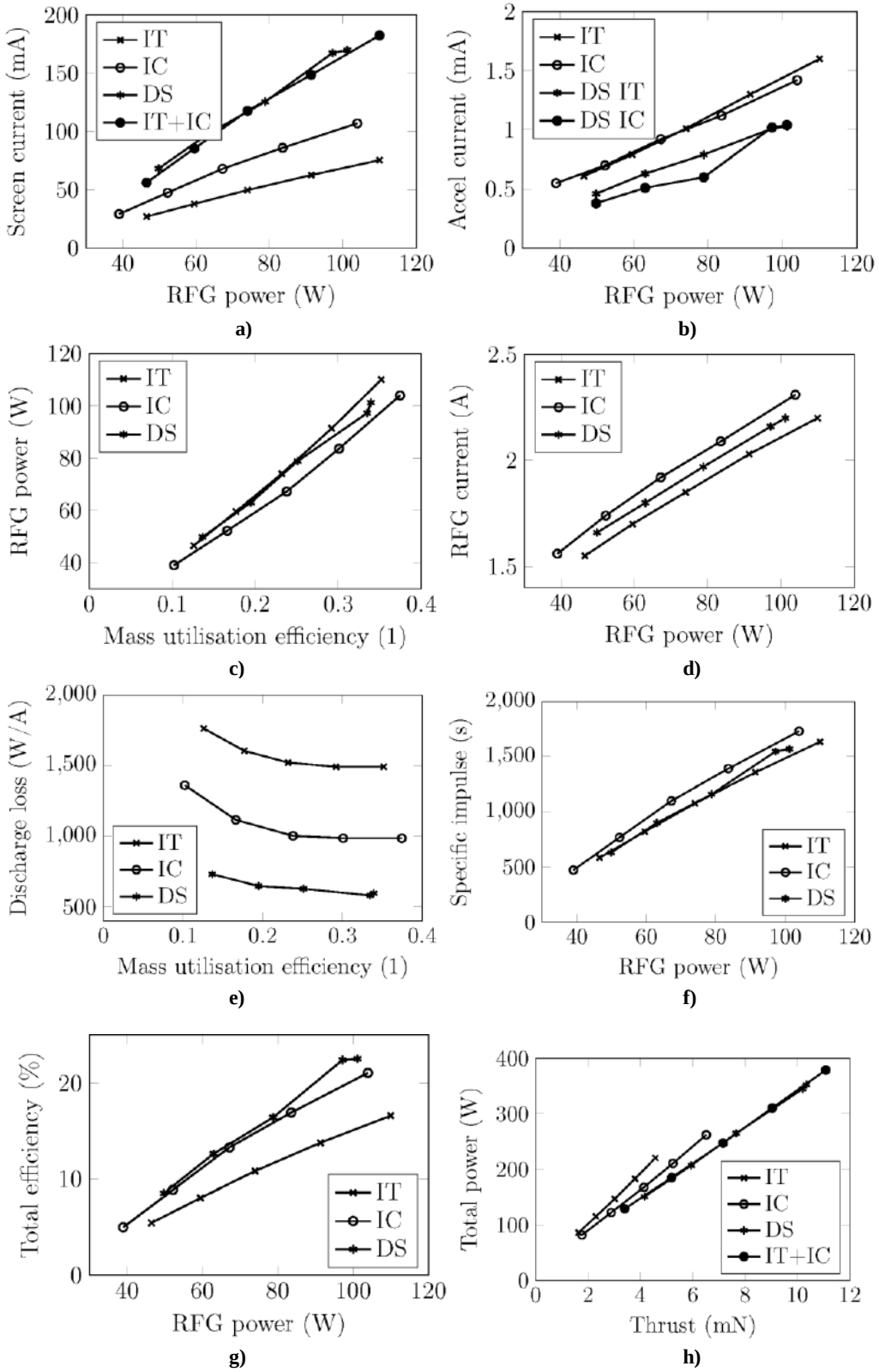

Figure 14. Performance parameters for Configurations AIT at 3 sccm, AIC at 4 sccm and ADST at 7 sccm (U_s=1.5 kV, U_{a1}=-250 V, U_{a2}=-150 V).

For instance, based on the Clausing[12] factors, it was calculated using the model developed in our previous[7] work, that regarding the plasma parameters, the thruster running at 7 sccm in Configuration ADST should be equal to the thruster operating at 4 sccm in Configuration AIC and 3 sccm in Configuration AIT. To check if this assumption is valid, Figure 14 compares the performance parameters as obtained by testing the AIT, AIC and ADST configurations at the above-mentioned mass flow rates. If the model results are correct, then the screen current measured in Configuration ADST (DS) should be about equal to the sum of currents measured in Configurations AIT and AIC (IT+IC). As can be seen from Figure 14(a), this indeed is the case. However, the IT and IC accel currents that were measured in Configuration ADST do not match the ones obtained in Configurations AIT and AIC, as shown in Figure 14(b). This could be due to slight differences in the number of the neutral gas atoms between the ion optics systems or in the sheath shapes. To reaffirm the previously stated theory, the RFG power variation with the mass utilization efficiency is plotted in Figure 14(c). Since the prediction has been made that the plasma parameters in both cases are about the same, all the cases should have nearly the same RFG power requirements for the same mass utilization efficiency values. This is precisely what can be seen in Figure 14(c). Additionally, the same should be expected by looking at the plot of the RFG current vs the RFG power in Figure 14(d). This is because due to the plasma parameters being similar, the RFG current should also be similar since the thruster's resistance in all the cases must be approximately the same.

The same explanation can also be used in predicting the specific impulse trends, as displayed in Figure 14(f). However, it can be observed from Figure 14(e) that the discharge loss obtained in Configuration ADST is about 400 W/A and 1,000 W/A smaller than those obtained in Configurations AIC and AIT, respectively. This is because even though the plasma is the same in all cases, Configuration ADST produces two ion beams and therefore the power to produce 1 mA is much lower. Figure 14(g) displays that the total efficiency in Configuration ADST is about the same as in Configuration AIC at low RFG powers. Nevertheless, the total efficiency becomes about a few percent higher as the RFG power goes past about 80 W. Finally, the thrust produced in Configuration ADST should be equal to a sum of thrusts produced in Configurations AIT and AIC. As depicted in Figure 14(h), this is in fact the case. As a result, it proves that the model results are correct and the plasma parameters are indeed the same at these flow rates. Therefore, it is possible to estimate the thrust produced by the IT and IC1 ion optics systems individually while the thruster is working at 7 sccm in Configuration DST. For instance, Figure 14(h) depicts that at the total power of 350 W, the IT thrust is about 4.1 mN while the IC thrust is about 6.3 mN, which is 54% more. Therefore, it can be concluded that Configuration ADST satisfies the LEOSWEEP mission requirements. That is, different thrust magnitudes can be produced from the IT and IC sides as required for the impulse transfer and impulse compensation, respectively. As mentioned before, this difference in the thrust magnitudes was controlled by having the ion optics systems with different numbers of apertures.

B. Configuration BDST

1. Performance mapping

The previous section was aimed at analyzing Configuration A. Remember that in Configuration ADST, the thruster had only one screen grid as a part of the IT ion optics system. In this section, however, Configuration BDST is investigated. In this configuration, there are screen grids located at each ion optics side. Also, the IC side has the IC2 ion optics system which consists of screen and accel grids made from titanium. Additionally, note that in Configuration B, the thruster was only operated in the double-sided mode. That is, both sides of the thruster were active. Figure 15 depicts the thruster firing in Configuration BDST. As can be seen, the beam from the IT side is not as wide and has a lower divergence compared to the beam from the IC side. Also, the IC2 ion optics system is not as bright as the IC1 ion optics system shown before since the titanium grids block all the light from the plasma.

As before, the performance mapping of the thruster was performed using the mass flow rates varying from 6 sccm to 14 sccm in 1 sccm increments. The screen grid voltage, however, was different compared to Configuration A. In Configuration BDST, the thruster was tested up to 2.5 kV. This is because the IC2 ion optics system could be operated between 1 - 2.5 kV without producing sparks. Additionally, there were two screen currents being recorded: I_s^{it} on the IT side and I_s^{ic} on the IC side. Figure 16(a) displays how both screen currents vary with the RFG power. First, notice that since the IC2 ion optics system has more apertures, the screen current is higher as well. For instance, at the RFG power of 100 W and 14 sccm, the electron current hitting the IT side screen grid is about 50 mA while that hitting the

IC side screen grid is nearly 90 mA. The trends, however, are almost identical to the ones observed in Configuration A.

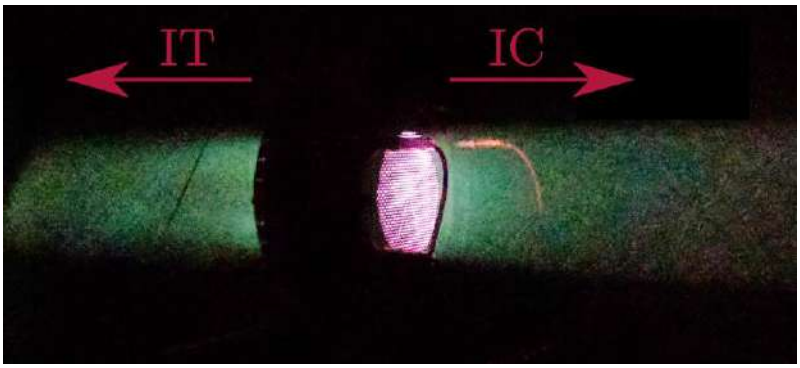

Figure 15. Extracted ion beams from the IT and IC2 ion optics systems in Configuration BDST.

Figure 16(b) shows the I_a^{it} and I_a^{ic} accel current variations for each ion optics side. As Figure 16(b) indicates, the IT side accel current is larger than that from the IC side throughout most of the operational points. For example, at the RFG power of 100 W and 14 sccm, the IT accel current is about 2.2 mA while the IC accel current is about 1 mA. This means that at these conditions the IC accel current is only about 1% of the extracted beam current. Finally, it can be seen in Figure 16(c) that the RFG current decreases with the mass flow rate, as was discussed before. Additionally, it can be observed that the RFG current is in the same range as for Configuration A. This means that, at the same RFG powers and mass flow rates, the plasma parameters remained nearly unchanged even though a new ion optics system was introduced.

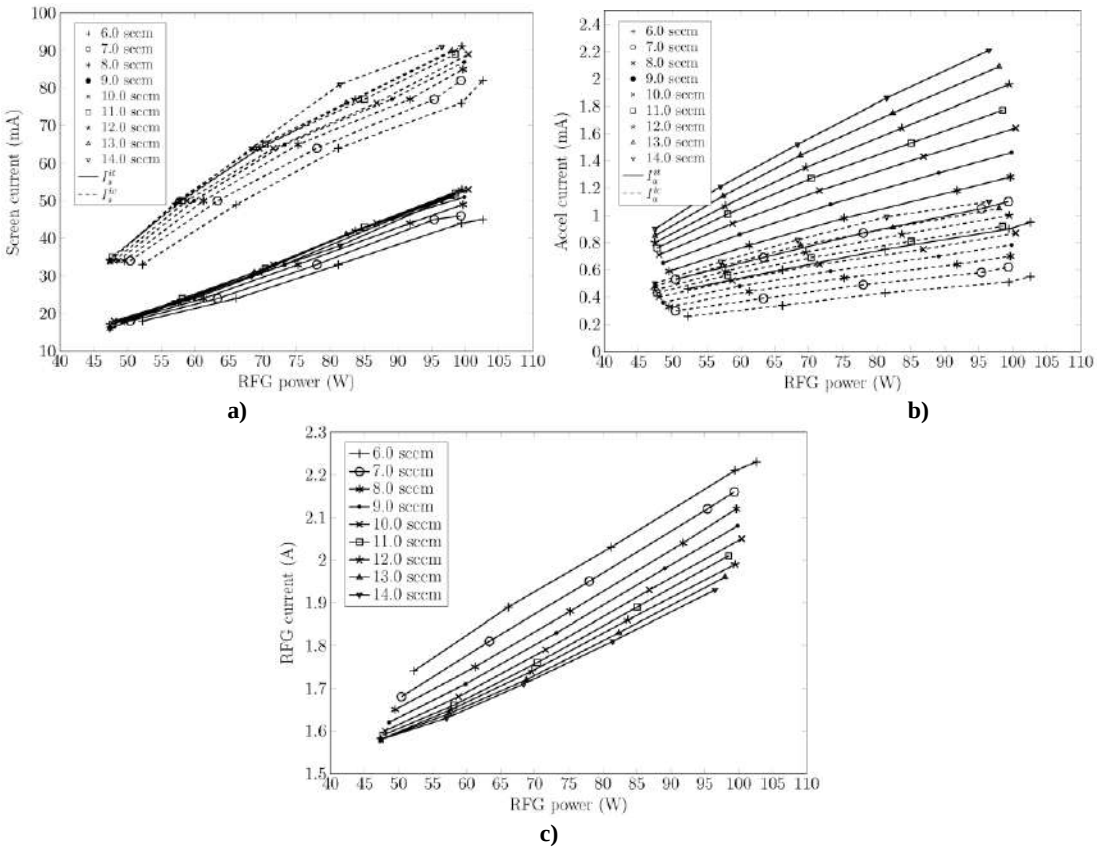

a) **b)**

c)

Figure 16. Configuration BDST: performance mapping at U_s=2.5 kV, U_{a1}=-250 V, U_{a2}=-150 V.

2. Performance analysis

The discussion regarding the performance analysis is started by depicting in Figure 17(a) how the discharge loss varies with the mass utilization efficiency. It can be seen, that the highest mass utilization efficiency achieved in Configuration BDST is equal to about 0.3 at 6 sccm. At this point, the discharge loss is about 800 W/A, which is about 150 W/A higher compared to Configuration ADST. This is because in Configuration ADST, a screen current that is about 50 mA greater compared to Configuration BDST was achieved. Figure 17(b) depicts that in Configuration BDST the maximum specific impulse obtained is about 1,800 s at 6 sccm. Note that such a specific impulse value is similar to that obtained in Configuration ADST. This is because even though the screen current obtained in Configuration BDST is lower than in Configuration ADST, in Configuration BDST, the screen voltage U_s is higher by 1 kV, which results in the specific impulse I_{sp} being higher as well since $I_{sp} \propto \sqrt{U_s}$. Furthermore, Figure 17(c) shows that the maximum total efficiency is about 20% at 100 W of RFG power and 6 sccm flow rate.

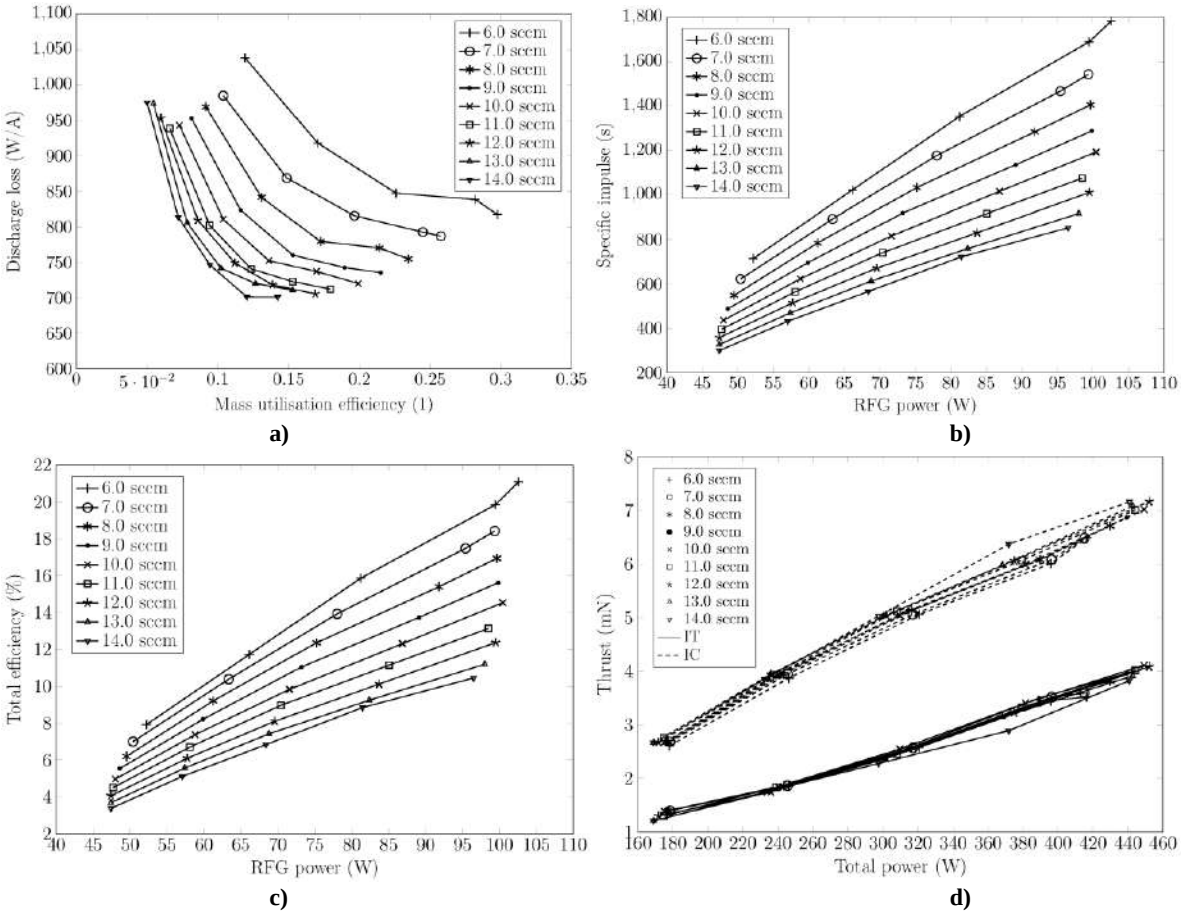

Figure 17. Configuration BDST: performance analysis at U_s=2.5 kV, U_{a1}=-250 V, U_{a2}=-150 V.

Finally, as Figure 17(d) depicts, in Configuration BDST, it is possible to predict the thrust magnitudes generated from each ion optics system because the exact IT and IC screen current values were recorded during the experiments. Figure 17(d) shows that the IC side constantly produces more thrust compared to the IT side. Additionally, depending on the operational conditions, the difference in the thrust values between the IT and IC sides varies from about 1 mN to 3 mN. For instance, at 440 W of total power and 9 sccm, the thrust achieved by the IC side is about 7 mN, while that from the IT side is approximately 4 mN. Therefore, the IC side produces 75% more thrust at these operational conditions. It can be concluded that since the IC2 ion optics system has a higher number of apertures it produces more thrust compared to the IT ion optics system, which is what has been observed in Configuration ADST.

C. Thrust control

1. Varying total power and mass flow rate

As discussed before, the IC side produces more thrust than the IT side. However, this difference in thrusts depends on the operating conditions. For instance, as the RFG power is altered, the plasma density changes and, as a result, the sheath shape and sheath parameters change. Therefore, since the ion optics systems are not the same, the focusing efficiency and perveance change and this influences the difference in thrusts. Nevertheless, this behavior of the thruster is actually beneficial. This is because it could happen that during the LEOSWEEP mission different ratios of the IC to IT thrust need to be produced. Therefore, Figure 18 displays how the thrust magnitudes from the IT and IC sides change with the mass flow rate and the total power. Notice that there are four trends plotted in total. The first two trends show the IC and IT side thrusts. The third trend shows the difference between the IC and IT thrusts given as IC-IT. This difference is important because it indicates how much thrust is produced to accelerate the thruster in one or the other direction. This is the key to the differential thrust control, as discussed by Collingwood[13]. Finally, the IC/IT-1 expression is also plotted to show (in percentage) by how much the IC thrust magnitude is larger (or smaller) than the IT thrust magnitude.

Figure 18(d) depicts that at 180 W of total power, the IC/IT-1 value is about 90%. However, as the total power increases, IC/IT-1 goes down to around 70% at about 450 W of total power. In the same figure, it can also be observed that the thrust difference IC-IT increases from about 1.3 mN at 180 W to about 3 mN at 450 W. The IC-IT value of 3 mN means that the satellite the thruster is attached to will effectively be subjected to 3 mN of force in the IT direction. This value again can be changed, by varying the total power and mass flow rate. For instance, Figure 18(h) shows that the IC thrust is about 120% higher than the IT thrust as the total power varies from 170 W to 380 W. By having the thruster's performance analyzed as in Figure 18, the best total power and mass flow rate depending on the mission requirements at a particular time can be chosen. If, for example, the IC to IT thrust ratio needs to be changed, the operator could change the total power or the mass flow rate until the required ratio is achieved. This allows for a lot of flexibility when designing an IBS type mission using the DST thruster.

2. Varying screen grid voltage

Another way to control the IC-IT and IC/IT-1 parameters is by changing the screen grid voltage in addition to changing the total power, as shown in Figure 19. This method results in much larger changes in the thrust values produced by the IT and IC sides. For instance, as can be seen in Figure 19(a), the IC/IT-1 value changes from about 80% at 106 W to 0% at 160 W. This means that at the power of 106 W both sides produce the same amount of thrust since IC-IT is equal to 0. Therefore, the satellite would not feel any acceleration. Such a wide range of IC/IT ratios is possible since at 1 kV, the ion beam produced by the IC ion optics system is not well focused (effective grid transparency is very low) and the ion beam is space charge limited at higher powers. Therefore, Figure 19(a) depicts that the IC thrust magnitude starts to decrease and is being overtaken by the IT thrust when the total power goes above 160 W.

Even though such a method of operating the thruster is very inefficient due to the poor focusing of one of the ion optics side beams, a very wide range of the IC/IT ratios is achievable. A similar behavior to that observed at the 1 kV case, is also displayed in Figure 19(b) at 1.5 kV. In this figure, even though the IC thrust is always increasing, the IT thrust overtakes the IC thrust at about 220 W, resulting in the IC/IT-1 parameter being negative. However, when the screen grid voltage goes above 2 kV, the beam focusing becomes much more efficient and the ion optics is no longer space charge limited. Therefore, the IC thrust is always higher than the IT thrust, and IC/IT-1 is always positive, as can be seen in Figure 19(c) and Figure 19(d). Note, however, that the beam currents from the IT and IC sides might be different than the corresponding screen currents as measured in the experiment. This is because it could happen that an electron, left behind an ion exiting the IT side, is collected by the IC side and vice versa. This would affect the results presented in this section. Therefore, plume parameter measurements are needed to be performed to determine the actual ion currents exiting the IT and IC sides.

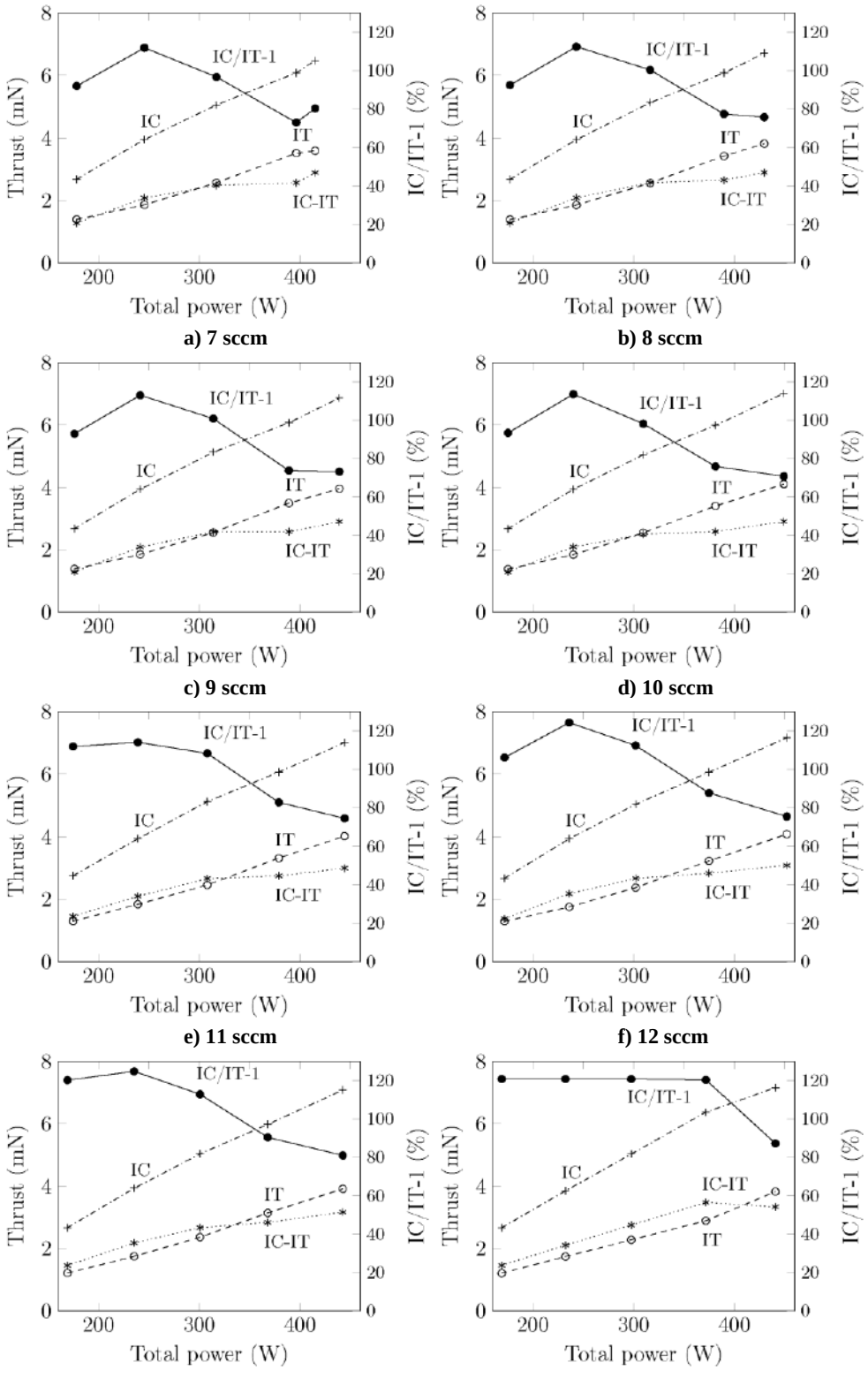

Figure 18. Configuration BDST: thrust variation for the IT and IC sides with total power and mass flow rate (U_s=2.5 kV, U_{a1}=-250 V, U_{a2}=-150 V).

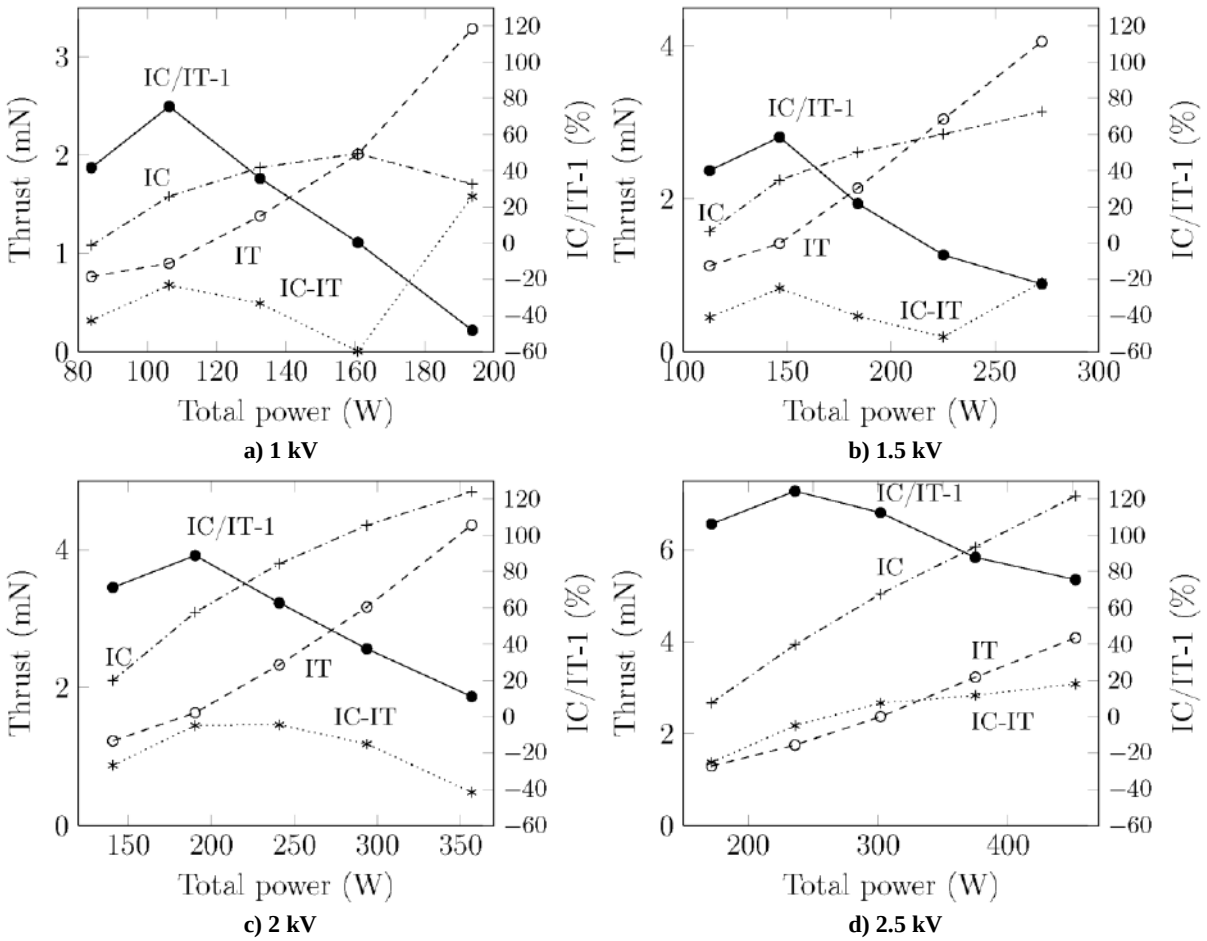

Figure 19. Configuration BDST: thrust variation for the IT and IC sides with the screen grid voltage at 12 sccm (U_{a1}=-250 V, U_{a2}=-150 V).

To better understand how the screen voltage affects the plasma parameters, the beam focusing and thus the thrust, the performance parameter variation with the screen grid voltage at 12 sccm flow rate is depicted in Figure 20. As shown in Figure 20(a), for high RFG powers, the IT screen current decreases as the screen voltage goes up. For instance, at approximately 100 W of RFG power, the screen current is 68 mA at 1 kV, while at 2.5 kV the screen current is 53 mA. In contrast, Figure 20 (b) depicts that the IC screen current increases as the screen voltage goes up. For instance, at about 100 W of RFG power, the screen current is 35 mA at 1kV, while at 2.5 kV the screen current is 91 mA. Such a discrepancy in the trends between the IT and IC currents is caused by the difference in the plasma parameters and the sheath shape as the screen grid voltage changes. Regarding the accel current, the IT accel current decreases substantially at high RFG powers and remains nearly unchanged at low RFG powers as the screen grid voltage increases, as shown in Figure 20(c). For instance, at about 50 W, the accel currents for all the screen grid voltage cases are approximately 0.8 mA. However, the difference in the accel currents at 100 W between 1 kV and 2.5 kV cases is about 1 mA. For the IC side, this is not the case, it seems that the accel current is not much affected by the change in the screen voltage, as seen in Figure 20(d).

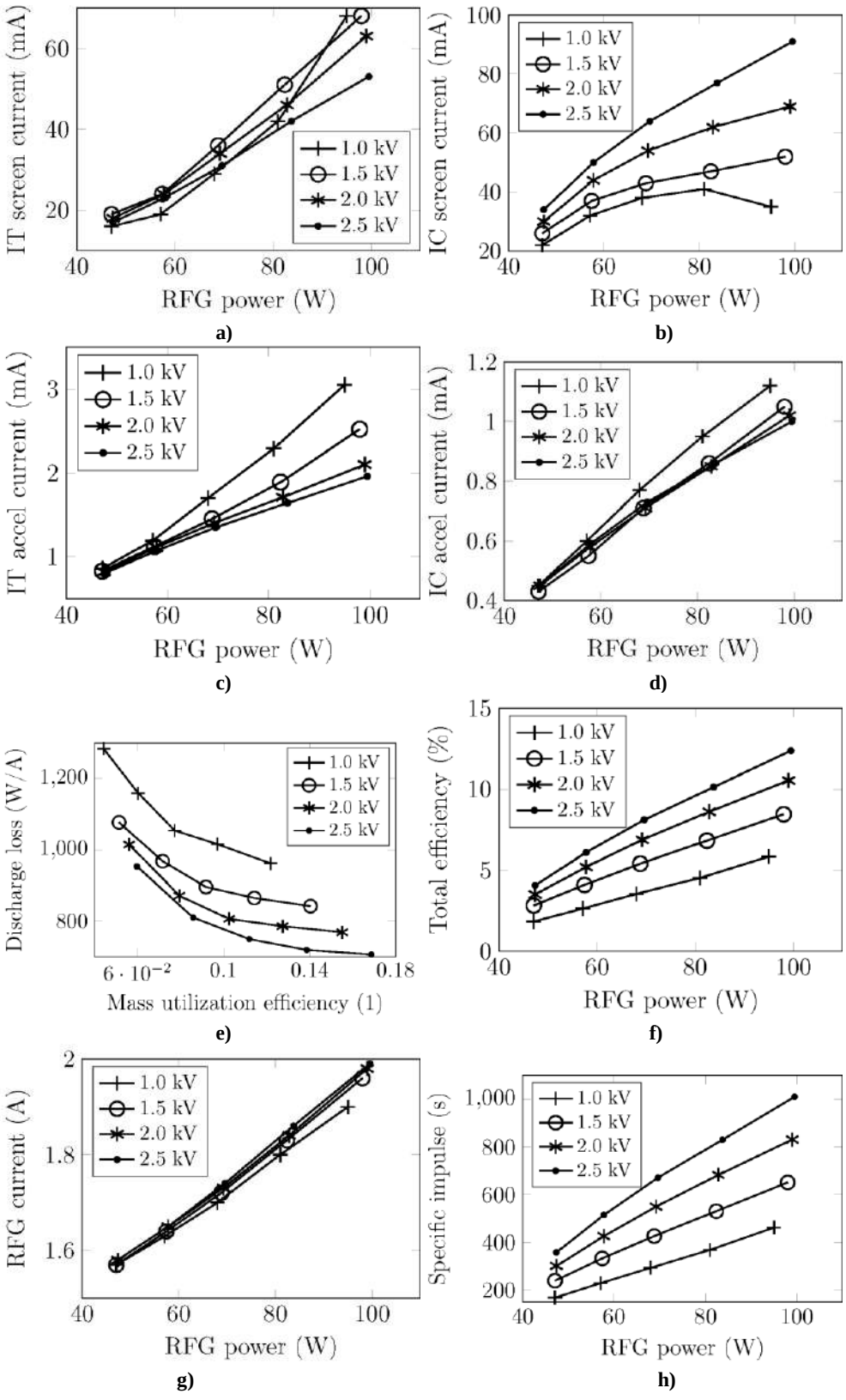

Figure 20. Configuration BDST: performance parameters vs RFG power at different screen grid voltages at 12 sccm (U_{a1}=-250 V, U_{a2}=-150 V).

Figure 20(e) depicts that as the screen voltage is increased, the discharge loss goes down significantly. For instance, at the mass utilization efficiency of 0.14, the discharge loss goes from about 900 W/A to about 700 W/A as the screen voltage increases from 1.0 to 2.5 kV, respectively. This is because the extracted beam currents go up with the screen voltage, as was shown before. Figure 20(f) indicates that the total efficiency also improves with the screen voltage. The total efficiency goes from about 5% to about 12% at 100 W of RFG power. Similarly, the specific impulse also increases from about 450 s to 1,000 s at 100 W of RFG power, as displayed in Figure 20(h). Finally, Figure 20(g) illustrates that the RFG current increases only by about 5% at the maximum as the screen voltage increases. This shows that the plasma parameters do not change significantly when the screen voltage changes. However, the change in the plasma parameters that does occur comes mainly from the reduced neutral gas pressure inside the discharge chamber as the screen current increases. This in turn causes a change in the ion density and the plasma sheath shape. Finally, the screen current is also affected by the screen grid voltage due to modification of the space charge limited current. As a result, the screen currents vary widely, as depicted in Figure 20(a) and Figure 20(b). Again, beam plume measurements are needed to confirm the exact beam currents. This would allow one to understand the exact relationship between the IT and IC screen currents.

3. Varying accel grid voltage

The final way to vary the IT and IC screen currents is to change the accel voltages. Figure 21 displays changes in various performance parameters with respect to a nominal accel voltage of 250 V for the IT case and 150 V for the IC case. It can be seen in Figure 21(a) that the change in the IT and IC side screen currents at 250 V is 0 since the thruster works at the nominal IT accel voltage. However, when the IT accel voltage is reduced to 0 V, the IT screen current decreases by nearly 1 mA, while the IC screen current goes down by about 0.2 mA. What is more, as displayed in Figure 21(a), by increasing the IT accel voltage to 400 V, both the IT and IC screen currents increase by about 0.5 mA. Furthermore, while changing the IT accel voltage, the IC accel current does not change, as shown in Figure 21(b). Nevertheless, the IT accel current decreases by about 0.4 mA when the IT accel voltage goes to 0 and increases by about 0.1 mA when the voltage goes to 400 V. Figure 21(c) depicts that the IT thrust changes from being lower by 40 µN at the IT accel voltage of 0 V to being higher by 30 µN at 400 V. Whereas, the IC thrust changes from being lower by 13 µN at the IT accel voltage of 0 V to being higher by 35 µN at 400 V. The change in the IC/IT-1 percentage value from the nominal is about 4% at the IT accel voltage of 0 V to almost no change at 400 V.

Furthermore, Figure 21(d) indicates that as the IC accel voltage goes up to 400 V, the IC screen current increases by 1.5 mA, while the IT screen current remains about the same. Upon reducing the IC accel voltage, the IC screen current remains unchanged, while the IT screen current increases by 1.5 mA. The IT accel current almost does not change with the IC accel voltage, as depicted in Figure 21(e). Whereas, the IC accel current increases by about 0.15 mA at 400 V, and decreases by about 0.15 mA at 0 V. Figure 21(f) shows that as the IC accel voltage is reduced to 0 V, the IT thrust increases by about 100 µN, while the IC thrust remains nearly the same. However, upon increasing the IC accel voltage to 400 V, the IT thrust remains unchanged, while the IC thrust increases by 100 µN. Finally, a variation in the change of the IC/IT-1 value from -12% to 6% occurs as the IC accel voltage is varied from 0 to 400 V, respectively. As has been shown, the IT and IC thrust values can be modified by changing the accel voltages. However, the maximum change is only about 100 µN. Therefore, the previously discussed changes in the screen grid voltage, RFG power and mass flow rate should be used for significant variation in the thrust values. However, changing the accel voltage should be employed for very fine thrust adjustments.

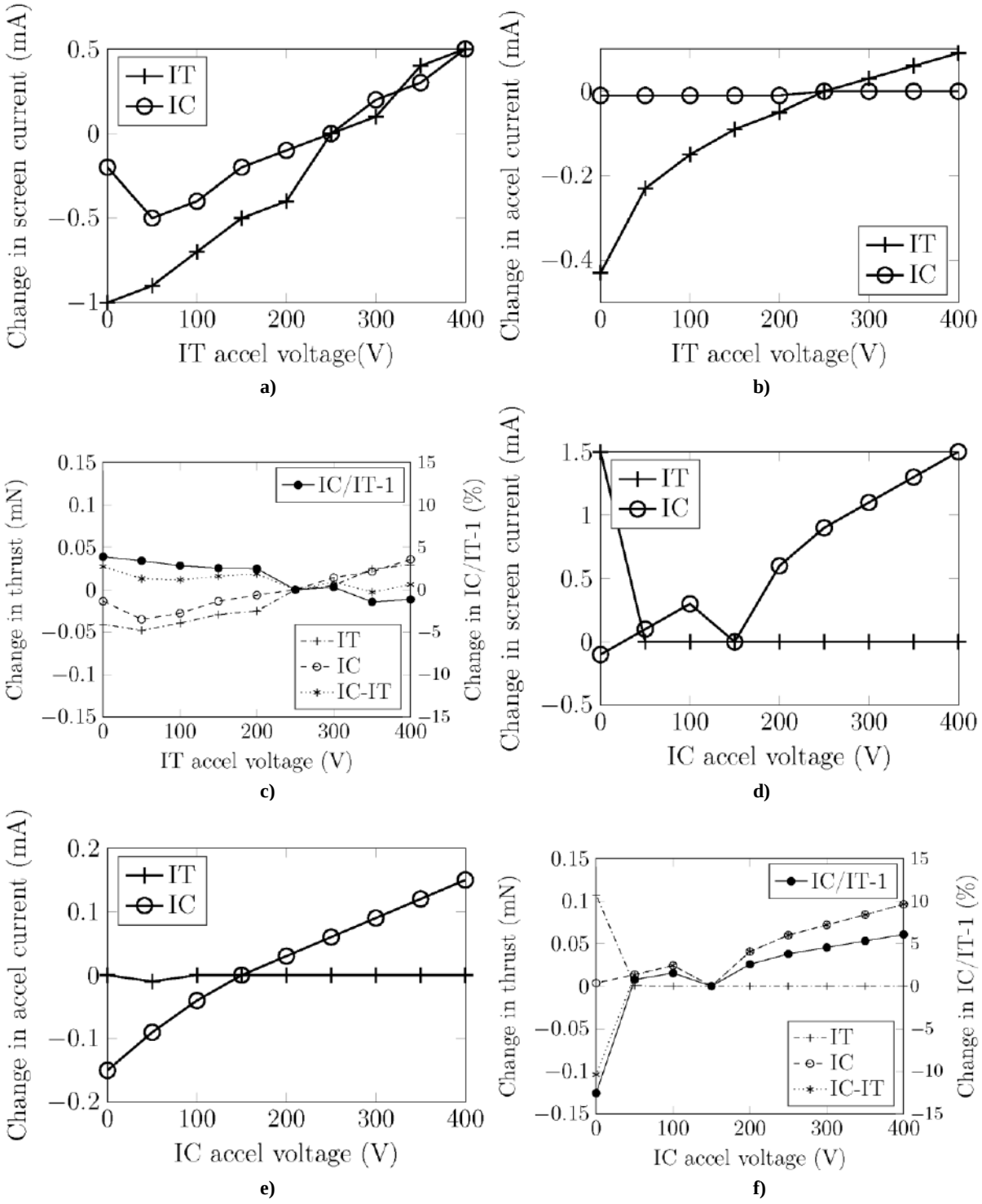

Figure 21. Configuration BDST: performance parameter variation for the IT and IC sides with the accel voltage at 10 sccm ($U_s = 2\ kV$). IT accel nominal voltage 250 V, IC accel nominal voltage 150 V. Note that all accel voltages are biased negatively (-).

IV. Conclusions

This paper has presented the experimental results obtained while testing the Double-Sided Thruster (DST) at the University of Southampton vacuum facility. The experimental campaign has shown promising results regarding the applicability of the double-sided thruster concept for the IBS type missions. In particular, two ion beams from the same discharge chamber have been extracted. Also, it was possible to achieve 30% more thrust from the IC ion optics side compared to the IT side, which was one of the LEOSWEEP mission requirements. This was achieved by designing the IC ion optics system with 24% more apertures than the IT ion optics system. During the experimental campaign, the thruster's performance was mapped by varying the mass flow rate, screen/accel grid voltages and the RFG power. However, while testing, only an RFG that goes to a maximum power of about 100 W was available. This meant that high mass utilization efficiencies could not be reached. However, 100 W of RFG power proved to be enough to validate the concept. Furthermore, it was assumed that the electron currents recorded in the IT and IC lines represent the beam currents. Nevertheless, this assumption is not entirely correct since it is possible that an electron left behind an ion exiting the IT ion optics side is collected by the IC ion optics side and vice versa. Therefore, in the future, beam plume measurements will be performed to determine exactly the IT and IC beam currents and to correlate these currents to the measured IT and IC screen electron currents.

For instance, the following parameters have been recorded during the experimental campaign for various configurations:

- Configuration AIT: IT thrust = 4.5 mN, screen voltage = 1.5 kV, total power = 210 W, mass utilization efficiency = 27%, specific impulse = 1,220 s, total efficiency = 13%;
- Configuration AIC: IC thrust = 6.5 mN, screen voltage = 1.5 kV, total power = 262 W, mass utilization efficiency = 37%, specific impulse = 1,730 s, total efficiency = 21%;
- Configuration ADST: IT thrust = 4.1 mN, IC thrust = 6.3 mN, screen voltage = 1.5 kV, total power = 350 W, mass utilization efficiency = 34%, specific impulse = 1,570 s, total efficiency = 22.5%;
- Configuration BDST: IT thrust = 3.6 mN, IC thrust = 6.5 mN, screen voltage = 2.5 kV, total power = 416 W, mass utilization efficiency = 26%, specific impulse = 1,545 s, total efficiency = 18.5%.

Furthermore, by analyzing the results, it was observed that the IT to IC thrust ratio (IC/IT-1) strongly depends on the mass flow rate, RFG power and the screen grid voltage. For instance, it was shown that the IC/IT-1 parameter varies from 120% to -50%. Therefore, the DST thruster could be suitable for a wide range of IBS mission scenarios. What is more, by varying the accel voltage it was possible to achieve changes in the IT and IC thrust magnitudes equal to about $\pm 100\,\mu N$. As a result, the accel voltage could be changed when fine thrust adjustments are needed. Nevertheless, the DST thruster presents a more limited range of the IC/IT thrust ratios compared to two single-sided thrusters. For instance, for some IBS type missions, it might be more desirable to have independent control of the IT and IC thrust magnitudes. Furthermore, during an IBS type mission, it could happen that some IC/IT thrust ratios cannot be reached using the DST thruster. Therefore, an IBS mission has to be designed keeping the available IC/IT thrust ratios as constraints. These constraints might increase the complexity/cost of the mission thus offsetting the benefits of the DST thruster. More research is still needed to determine the throtability limits of a double-sided thruster before its full potential for the IBS type missions can be ascertained.

References

[1]Bombardelli, C. and Peláez, J., "Ion Beam Shepherd for Contactless Space Debris Removal," Journal of Guidance, Control and Dynamics, 34(3), 2011, pp. 917-920.

[2]Merino, M., Ahedo, E., Bombardelli, C., Urrutxua, H. and Peláez, J., "Space Debris Removal with an Ion Beam Shepherd Satellite: Target-Plasma Interaction," presented at the 47th AIAA/ASME/SAE/ASEE Joint Propulsion Conference & Exhibit 31 July – 03 August, San Diego, California, 2011.

[3]Ruiz, M., Urdampilleta, I., Bombardelli, C., Ahedo, E., Merino, M. and Cichocki, F.,"The FP7 LEOSWEPP Project: Improving Low Earth Orbit Security with Enhanced Electric Propulsion," presented at the Space Propulsion 2014 Conference, Cologne, France, 2014.

[4]Cichocki, F., Merino, M., Ahedo, E., Feili, D. and Ruiz, M., "Electric Propulsion Subsystem Optimization for "Ion Beam Shepherd" Missions," presented at the 30th ISTS, 34th IEPC and 6th NSAT Joint Conference, Hyogo-Kobe, Japan, 2015.

[5]Dobkevicius, M., Feili, D., Smirnova, M., and Mingo, A., "Double-Sided Ion Thruster for Contactless Space Debris Removal," presented at the Space Propulsion 2016 Conference, 02-06 May, Rome, Italy, 2016.

[6]Dobkevicius, M., "Modelling and Design of Inductively Coupled Radio Frequency Gridded Ion Thrusters with an Application to Ion Beam Shepherd Type Space Missions," in Ph.D. Thesis, Southampton, UK, University of Southampton, 2017

[7]Dobkevicius, M., Feili, D. and Muller, J., "Comprehensive Radio – Frequency (RF) Ion Thruster Electromagnetic and Thermal Modelling," presented at the 30th ISTS, 34th IEPC and 6th NSAT Joint Conference, Hyogo-Kobe, Japan, 2015.

[8]Chabert, P. and Braithwaite, N., *Physics of Radio-Frequency Plasmas*, Cambridge University Press, Cambridge, 2011.

[9] Feili, D., Smirnova, M. Dobkevicius, M., and et al., "Impulse Transfer Thruster for an Ion Beam Shepherd Mission," presented at the 30th ISTS, 3th IEPC and 6th NSAT Joint Conference, Hyogo-Kobe, Japan, 2015.

[10]Sico, Sico Technology is Producing Two Types of Quartzglass, htttp://www.sico.at/en/quartz.html [accessed: 2017-01-15].

[11]Dobkevicius, M.," Dataset for Double-Sided Thruster (DST) Experimental Data," University of Southampton doi:10.5258/SOTON/405417, 2017.

[12]Clausing, P., "The Flow of Highly Rarified Gases Through Tubes of Arbitrary Length," Journal of Vacuum Science and Technology, 1971, 8(5):636-646.

[13]Collingwood, C.," Investigation of a Miniature Differential Ion Thruster," in Ph.D. Thesis, Southampton, UK, University of Southampton, 2011.